

Thermotropic Mesomorphism of a Model System for the Plant Epicuticular Wax Layer

Laura Carreto,* Ana Rita Almeida,* Anabela C. Fernandes,[†] and Winchil L. C. Vaz*

*Departamento de Química, Universidade de Coimbra, 3004-535 Coimbra, Portugal; and [†]Departamento de Engenharia Química, Instituto Superior Técnico, 1049-001 Lisboa, Portugal

ABSTRACT As a model for the epicuticular wax layer of plant cuticular membranes, we have studied the phase behavior of 1-tetradecanol and 1-octadecanol and their binary mixtures between 5 and 70°C, using differential scanning calorimetry and Fourier transform infrared spectroscopy (FTIR). Both pure compounds show two exothermic phase transitions corresponding to a transformation from a liquid phase to a hexagonally packed solid phase (S_{HEX}), which at lower temperatures transforms to an orthorhombically-packed solid phase (S_{ORT}). On heating the S_{ORT} solid a single endothermic transition with a transition enthalpy corresponding to the sum of the exothermic transition enthalpies is obtained. These transitions were also followed using FTIR spectroscopy in the CH_2 -stretching (symmetric and asymmetric) and CH_2 -rocking vibration modes. The FTIR spectra of the pure compounds in the liquid, S_{HEX} , and S_{ORT} phases were used to simulate experimental spectra in the phase transition regions. The simulations allowed us to estimate the molar fractions of each phase in the transition regions of the pure compounds. A phase diagram for the binary mixture of 1-tetradecanol and 1-octadecanol was obtained using differential scanning calorimetry and FTIR. FTIR studies on binary mixtures prepared from one perdeuterated component and the other nondeuterated permitted studying the thermotropic behavior of each component in the mixture independently. The mixture shows an eutectic behavior with an eutectic point between a molar fraction of octadecanol (X_{18}) of 0.12 and 0.18 and a temperature of $\sim 32^\circ\text{C}$. Below 32°C , a binary mixture of solid phases, one an S_{ORT} phase and the other an S_{HEX} phase, coexist up to $\sim 25^\circ\text{C}$, below which both solid phases are S_{ORT} phases. We discuss the possible relevance of this complex phase behavior in a simple binary mixture of two long-chain alkanols in the context of the far more complex phase behavior expected for the plant epicuticular wax layer.

INTRODUCTION

The epidermal cell layer of the tender aerial parts of higher plants is covered by a cuticular membrane, which constitutes an effective barrier against desiccation. When plant stomata are closed or absent, gaseous exchanges between the plant and the atmosphere occur across the cuticular barrier. In addition to the loss of water by transpiration, permeation into the plant of chemicals deposited on its surface is dependent on the transport properties of the cuticle (Schreiber et al., 1996).

The cuticle consists of a polymer matrix of long-chain polyesters, the cutin, in which waxes are embedded and deposited on the external surface. Cuticular wax composition can be quite complex and varies greatly according to species, age, and environmental conditions. *n*-Alkanes and primary *n*-alkanols with chain lengths ranging from C_{16} to C_{36} are important and in many cases are the predominant lipid species in epicuticular waxes (Holloway, 1994).

A generally accepted model for cuticular permeation is based on a partition-diffusion-desorption mechanism where

the rate limiting factors for permeation are the wax-aqueous phase partition coefficient, K_p , and the diffusion coefficient, D ($\text{m}^2 \text{s}^{-1}$), of the compound within the cuticular wax layer. According to the studies of several authors (reviewed by Schreiber et al. (1996)), the transport across the cuticle is essentially determined by the wax composition. However, although the physical properties of the wax layer are dependent upon wax composition, a simple relationship between wax physical state and barrier properties of the cuticle (Schreiber and Riederer, 1996) has not yet been clearly established.

To understand the barrier properties of the plant cuticle, it is necessary to understand the physical state of the cuticular wax layer. Considering the compositional complexity, it cannot, a priori, be expected to be a homogeneous system. A model of the physical structure of the epicuticular wax layer proposed by Reynhardt and Riederer (1991) describes it as a matrix composed of highly ordered crystalline and disordered “amorphous” regions. Reduced diffusional dynamics in the crystalline regions of the wax barrier make them practically inaccessible to permeation. Thus, a large fraction of the total volume of the barrier is effectively excluded for transport, which may be expected to occur only through the noncrystalline regions. More than its chemical composition, the physical state of the wax layer may be the determinant feature in the transport properties of the cuticle.

The physical state of a mixture, as a function of its chemical composition and physical variables (temperature, pressure, etc.), is best understood by establishing a phase

Received for publication 19 January 2001 and in final form 26 September 2001.

Laura Carreto is on study leave from Área Departamental de Química, Faculdade de Ciências e Tecnologia, Universidade do Algarve, Campus de Gambelas, 8000 Faro, Portugal.

Address reprint requests to Prof. Winchil Vaz, Departamento de Química, Universidade de Coimbra, 3004-535 Coimbra, Portugal. Tel. 351-239-824861; Fax: 351-239-827703; E-mail: wwaz@ci.uc.pt.

© 2002 by the Biophysical Society

0006-3495/02/01/530/11 \$2.00

diagram for it. Phase diagrams of mixtures as complex as the epicuticular wax layer are difficult, if not practically impossible, to obtain and, in any case, are not very informative due to their complexity. However, phase diagrams of binary or ternary mixtures are much simpler and often provide information that permits their use as simple models for understanding the behavior of much more complex mixtures. In the present work we have examined the phase diagram of a binary mixture of 1-tetradecanol and 1-octadecanol as a model system for the epicuticular wax layer. The known polymorphism of long alkyl chain compounds (McClure, 1968) and the natural abundance of *n*-alkanols in the epicuticular waxes of some drought resistant species (Reynhardt and Riederer, 1991; Martins et al., 1999) make the understanding of such a mixture, as a model, attractive.

Long-chain primary alcohols exhibit solid-state polymorphism, observed previously by x-ray diffraction studies and thermal analysis (Watanabe, 1961; Davies and Kybett, 1965a,b; Pradhan et al., 1970; Mosselman et al., 1974; Kuchhal et al., 1979). In this work we report on the thermotropic polymorphism of pure 1-tetradecanol and pure 1-octadecanol and binary mixtures of the two. The polymorphism was studied by differential scanning calorimetry (DSC) and Fourier transform infrared spectroscopy (FTIR). Both pure compounds as well as their mixtures show the existence of more than one solid phase and a high-temperature liquid phase, which in the mixtures may coexist over a wide range of temperatures. The polymorphism of the binary mixture of *n*-alkanols studied will be discussed on the basis of the experimental results and in the context of its relevance to the transport properties of an epicuticular wax layer.

MATERIALS AND METHODS

1-Tetradecanol and 1-octadecanol (both of analytical grade) were purchased from Sigma-Aldrich Co. (Madrid, Spain) and used without further purification. The purity of the alcohols was checked by gas chromatography analysis and found to be 99.3% for 1-tetradecanol and 99.6% for 1-octadecanol. Perdeuterated 1-tetradecanol-D₂₉ and 1-octadecanol-D₃₇ (both 98% pure) were obtained from Larodan Fine Chemicals (Malmö, Sweden) and used without further purification.

DSC measurements

DSC measurements were carried out on a Setaram DSC121 calorimeter (Caluire, France) with continuous purge of the reference and sample compartments with Argon. The calorimeter was periodically calibrated for temperature and heat-flow measurements with Indium as reference at a scanning rate of 1°C min⁻¹, according to the standard procedures described in the user's manual.

Binary mixtures of 1-tetradecanol + 1-octadecanol were prepared by sealing, in the same aluminum crucible, the appropriate amounts of the alkanols (weighed to a precision of ±0.01 mg on a Mettler microbalance) with the total mass not exceeding 7 mg. Before sealing the crucible, the alkanols were manually stirred with a metal wire to facilitate the mixing of the two components. Initially, samples were heated at 2°C min⁻¹ up to 100°C, annealed in the molten state for 5 min, and cooled to the desired

temperature at a rate of 1°C min⁻¹. Samples were then subjected to three consecutive heating and cooling cycles at a scanning rate of 1°C min⁻¹. In general, the second and third cycles were coincident. The last heating/cooling cycle was used for the determination of the transition temperatures and enthalpies. Selected mixtures were prepared three times, *ab initio*, and were found to give essentially identical results.

The molar enthalpies of transition were calculated by integration of the peak areas in the thermograms using the Setaram DSC-analysis software. The transition temperatures for the pure alkanols were determined from the thermograms as the onset temperature of the peaks, defined as the intersection of the baseline with the tangent to the peak shoulder. The onset and completion temperatures of a transition were obtained from the thermograms as the temperatures of departure and return to the baseline, respectively.

FTIR measurements

The pure alkanols (weighed to a precision of ±0.1 mg on a Mettler microbalance) were melted on a glass plate at ~70°C and maintained at this temperature for 5 min. An aliquot of the molten sample was placed between two potassium bromide windows preheated at the same temperature, and a slight pressure was applied to obtain a thin sample film. Mixtures of alkanols were prepared for FTIR measurements by first melting the appropriately weighed constituents of the mixture together at a temperature of 100°C and leaving overnight at this temperature. The sample was then cooled to ~10°C and subjected to two consecutive heating and cooling cycles between that temperature and 100°C after which they were left at 10°C for 48 h. An aliquot of the powdered solid sample was placed between two KBr windows and gently compressed to yield a thin sample film. FTIR spectra were acquired with samples that had absorbance values below 1.5 units. For temperature scans, a thermocouple connected to a thermostat was placed in the sample window close to the sample. Spectra were recorded on a Bomem MB-104 spectrophotometer (Quebec, Canada). The spectral resolution used was 4 cm⁻¹. Sixteen scans were added per sample spectrum, and Fourier transformation of the spectra was done using the Win Bomem Easy 3.5 software package. Typically, the spectra were obtained at intervals of 1°C allowing 1 min for temperature equilibration after the required temperature had been attained. The temperature scale of the FTIR experiments was calibrated relative to the DSC temperature scale by matching the transition onset temperatures for the melting of a series of long-chain *n*-alkanols with chain lengths from C₁₂ through C₂₂ (melting temperatures between 20 and 70°C). For baseline correction in the FTIR spectra, a line passing through the coordinates of the points at 1805.2 and 4000 cm⁻¹ was subtracted from the whole spectrum. Subsequently, all spectra were normalized using Origin 5.0 software package (MicroCal Software, Northampton, MA). The positions of the vibration bands were determined using the peak picking routine of the Win Bomem Easy 3.5 software package.

RESULTS

DSC measurements on the pure alkanols

The thermal behavior of pure 1-tetradecanol and pure 1-octadecanol was first studied by DSC. Typical heating and cooling scans are shown in Fig. 1. Thermograms obtained on heating the solid samples showed a single endothermic transition for each case with the onset temperature for melting of octadecanol ~20°C higher than that for tetradecanol. The inverse process, i.e., cooling of the samples, showed two exothermic transitions, both asymmetric with onset temperatures differing only by a few degrees in each

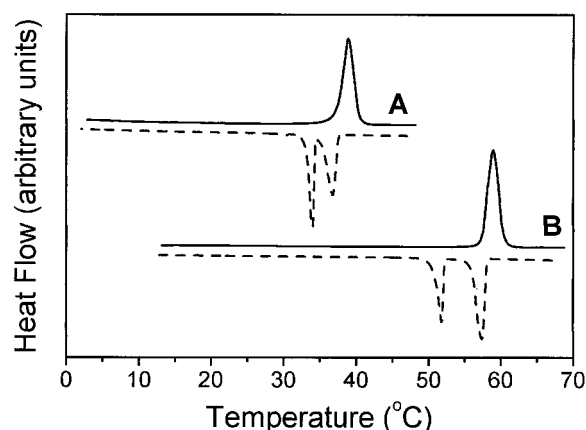


FIGURE 1 DSC thermograms obtained for the melting (solid line) and crystallization (dashed line) of 1-tetradecanol (A) and 1-octadecanol (B).

case. Again, the crystallization process for octadecanol is shifted to higher temperatures by $\sim 20^\circ\text{C}$ relative to that for tetradecanol. The first of the two peaks corresponds to the liquid-solid transition from which the crystallization temperature (T_c) and the molar enthalpy of the transition (ΔH_c) could be obtained. The second peak was attributed to a transition from one solid state to another with the transition temperature and molar enthalpy being designated by T_t and ΔH_t , respectively. The onset temperature of the melting transition is similar in both cases to the onset temperature of the first transition observed in the cooling process (Fig. 1). The transition temperatures and molar enthalpies for the endothermic (melting) and exothermic (crystallization) processes of the pure *n*-alkanols are listed in Table 1.

Comparing the heating and cooling thermograms of both alkanols, it is evident that the completion of melting is consistently at a higher temperature than the corresponding onset of crystallization. Ideally, the onset temperature of the crystallization and the completion temperature of the melting should be coincident if the cooling and heating rates are sufficiently slow to allow equilibrium conditions. In fact, the hysteresis could be slightly reduced when the temperature scanning rate was $0.2^\circ\text{C min}^{-1}$ instead of 1°C min^{-1} but was still of $\sim 2^\circ\text{C}$. The melting curve of 1-octadecanol showed the occurrence of two, albeit poorly resolved, transitions when the scanning rate was $0.2^\circ\text{C min}^{-1}$, but the

same was not observed for 1-tetradecanol (results not shown).

Long-chain *n*-alkanes and similar compounds, including *n*-alkanols, are known to freeze from an isotropic liquid phase (L) to a solid phase at a characteristic temperature T_c . The resulting solid phase (S_{HEX}) has a hexagonal packing symmetry and rotational freedom of the chains about their long axes (McClure, 1968). In the case of long chain 1-alkanols, the S_{HEX} phase has been reported to be metastable (Watanabe, 1961). A further transition at a slightly lower temperature, designated T_t , involves a rearrangement to a second solid phase (S_{ORT}) with orthorhombic packing without rotational freedom of the chains (McClure, 1968). This solid→solid transition has been observed for *n*-alkanols using different techniques (Watanabe, 1961; Pradhan et al., 1970; Mosselman et al., 1974; Kuchhal et al., 1979). All these different physical states are characterized by inter-chain interactions, which are reflected in the vibration spectra (infrared and Raman) through intermolecular coupling of the vibration modes (Casal et al., 1982). We, therefore, further investigated the thermotropic polymorphism of the alkanols and their mixtures by FTIR.

In the literature referring to the polymorphism of *n*-alkanols, it has been common practice to refer to the hexagonal solid phase with rotational freedom of chains as the α form and to the orthorhombic solid phase as the β form. Because the hexagonal and orthorhombic phases described for *n*-alkanols have properties that are very similar to those of the *n*-alkanes and the vibrational spectra obtained by us for the pure *n*-alkanol phases are equivalent to the vibration spectra for *n*-alkanes reported by Casal et al. (1982, 1983), we have opted to use the more descriptive S_{HEX} (for the α phase) and S_{ORT} (for the β phase) notation in this work.

FTIR measurements on the pure alkanols

The detailed infrared spectroscopic behavior of the various *n*-alkane phases has been described by Mantsch and collaborators (see Casal et al., 1982, 1983; Casal and Mantsch, 1984, and references cited therein). We have used the results of these authors to interpret the temperature dependence of the FTIR spectra of the 1-alkanols and their binary mixtures studied by us in this work.

FTIR spectra of both pure *n*-alkanols exhibited the typical bands of the CH_2 -stretching ($2800\text{--}3000\text{ cm}^{-1}$) and CH_2 -rocking ($700\text{--}750\text{ cm}^{-1}$) vibration modes reported for polymethylene chains and also the intense broad band corresponding to the OH stretching vibration around 3300 cm^{-1} (Fig. 2). At low temperatures below the onset of the melting transition, the S_{ORT} phase is characterized by the existence of two bands in the CH_2 -rocking vibration mode region ($720\text{--}750\text{ cm}^{-1}$). On heating, this phase transforms at T_m to an L phase, which results in a coalescence of these bands, the high frequency component no longer being apparent in the spectra. The CH_2 -stretching vibration mode region

TABLE 1 Transition characteristics of 1-tetradecanol and 1-octadecanol

Alkanol	T_m^* ($^\circ\text{C}$)	T_c^\dagger ($^\circ\text{C}$)	T_t^\dagger ($^\circ\text{C}$)	ΔH_m^* (kJ mol^{-1})	ΔH_c^\dagger (kJ mol^{-1})	ΔH_t^\dagger (kJ mol^{-1})
1-Tetradecanol	37.1	37.6	34.5	45.4	23.9	21.5
1-Octadecanol	57.1	58.0	52.1	64.2	39.9	23.6

*Obtained from the heating thermograms.

†Obtained from the cooling thermograms.

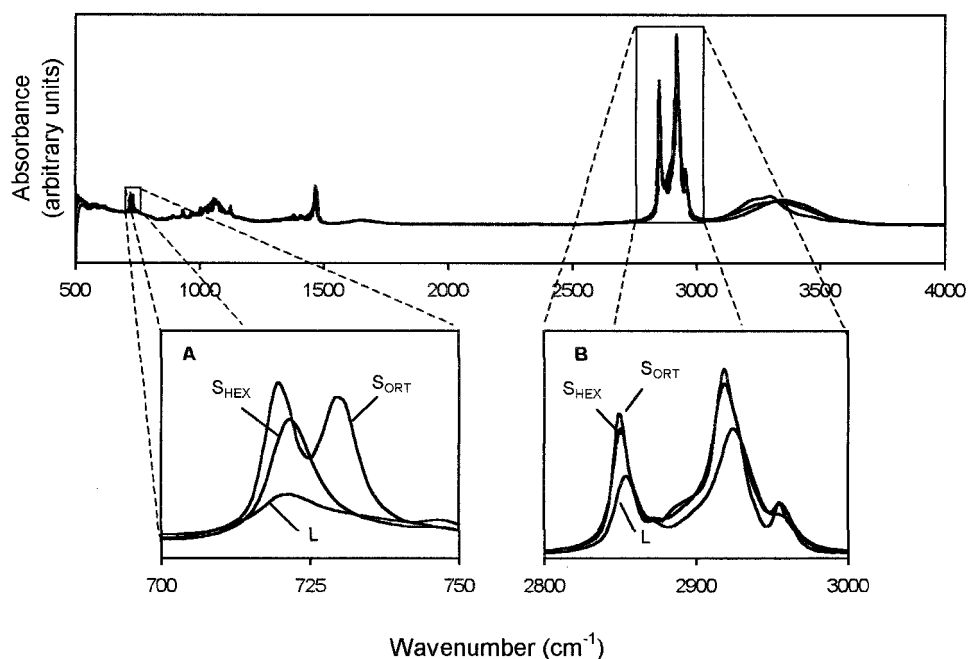


FIGURE 2 FTIR spectra of 1-tetradecanol in the L (46°C), S_{HEX} (37°C), and S_{ORT} (28°C) phases during a typical cooling run. (A) Spectra in the CH_2 -stretching (symmetric and asymmetric) frequency region; (B) spectra in the CH_2 -rocking frequency region.

(2800–3000 cm^{-1}) also shows the changes in absorbances and band frequencies expected (Fig. 2). In cooling scans, at temperatures above T_c , the spectral regions corresponding to CH_2 -rocking (700–750 cm^{-1}) and CH_2 -stretching (2800–3000 cm^{-1}) vibration modes showed bands typical of polymethylene chains in the liquid state. Just below T_c a shift to lower frequencies and an increase in intensity of the CH_2 -stretching vibration bands becomes evident. This shift is more pronounced for the $L \rightarrow S_{\text{HEX}}$ phase transition at T_c than for the $S_{\text{HEX}} \rightarrow S_{\text{ORT}}$ transition at T_t . Both transitions are also clearly manifested in the CH_2 -rocking band as an increase in the 720 cm^{-1} band intensity, diagnostic of an $L \rightarrow S_{\text{HEX}}$ transition (at T_c), and band-splitting and corresponding intensity changes upon the $S_{\text{HEX}} \rightarrow S_{\text{ORT}}$ solid phase transition at T_t . In particular, the band splitting is a very clear indication of the existence of the S_{ORT} solid phase. The results are summarized in Fig. 3. The onset and completion temperatures of the transitions seen in the FTIR spectra are equivalent to those seen by DSC (Fig. 1 and Table 1).

It should be pointed out that the S_{HEX} phase is metastable and converts to the S_{ORT} phase upon annealing the samples at a temperature between T_c and T_t . The kinetics of the process are slower for longer chain n -alkanols. Thus, for example, the S_{HEX} phase annealed to an S_{ORT} phase at a temperature immediately below the completion temperature of the $L \rightarrow S_{\text{HEX}}$ transition within approximately an hour in the case of 1-tetradecanol, over several hours in the case of 1-octadecanol, and did not anneal to the S_{ORT} phase over 1

day in the case of 1-docosanol (unpublished results). We are currently investigating the annealing process in more detail.

Using the vibrational spectra (obtained experimentally) at temperatures $\sim 5^\circ\text{C}$ above T_c as characteristic for the L phase, at temperatures $\sim 2^\circ\text{C}$ below T_c as characteristic for the S_{HEX} phase, and at temperatures $\sim 5^\circ\text{C}$ below T_t as characteristic for the S_{ORT} phase, it was possible to simulate the experimental spectra at all temperatures examined. For this simulation the experimental spectrum at a given temperature was considered to be a simple arithmetic composite of the three characteristic spectra each weighted by its fractional mass. The difference between the simulated composite spectra and the experimental spectra was less than 1% at any given frequency. The fractional masses of each phase as a function of temperature could be obtained for the pure compounds from this simulation (data not shown).

DSC-analysis of binary mixtures of 1-tetradecanol and 1-octadecanol

The thermal behavior of the 1-tetradecanol + 1-octadecanol binary mixture was first investigated by DSC. Heating and cooling thermograms were obtained at a scanning rate of $1.0^\circ\text{C min}^{-1}$. The heating thermograms were found to be consistently different from those obtained during the cooling, both in the number and in the position of the endothermic and exothermic peaks. As in the case of the pure components, the completion of melting was always observed to occur at higher temperatures relative to onset of

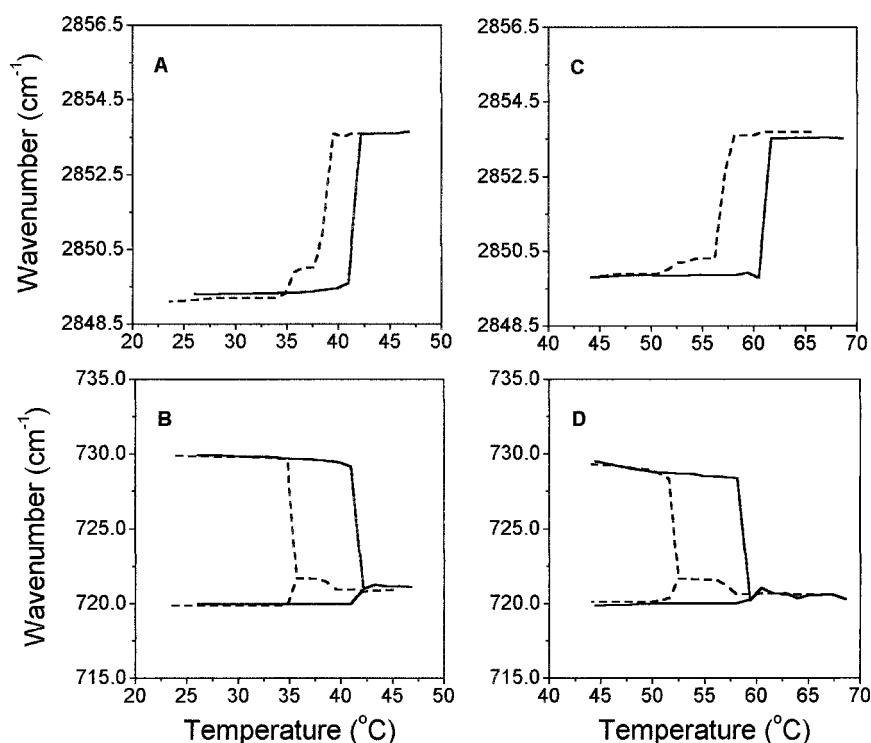


FIGURE 3 CH₂-stretching and CH₂-rocking vibration band frequencies observed for the melting (solid line) and crystallization (dashed line) of 1-tetradecanol (A and B) and 1-octadecanol (C and D) as a function of temperature.

crystallization. However, the molar enthalpies calculated for the total of the exothermic transitions equaled that of the endothermic transitions (within $\pm 5\%$ in 23 mixtures), showing that the melting and crystallization processes were completely reversible and completed within the monitored temperatures. Several heating scans, which were used in the definition of the phase diagram of the binary mixture, are shown in Fig. 4.

Mixtures with molar compositions very close to purity showed one endothermic peak similar to that observed for the pure components. In most of the compositions, however, the phase transition was only completed with several, partially superimposed, endothermic transitions occurring over a large range of temperatures. The onset and completion temperatures for the melting of the mixtures were obtained from the heating thermograms and were used to construct the phase diagram shown in Fig. 5. The diagram has the general form of an eutectic with a minimum in the liquidus line between molar compositions of $X_{18} = 0.12$ and $X_{18} = 0.18$. The liquidus line predicted from ideal solubility considerations, using the values of T_m and ΔH_m derived from the endothermic peak corresponding to the transition properties of the $S_{ORT} \rightarrow L$ transition of the pure compounds (see Table 1), is plotted as a dashed line in Fig. 5. In this regard it is interesting to note that we observe a minimum in the total molar enthalpy of the transitions (data not shown) at $X_{18} \approx 0.15$. The differences between ideal solubility pre-

dictions and experimental results are particularly evident for mixtures of molar composition between $X_{18} = 0.23$ and $X_{18} = 0.40$. To investigate whether this deviation was a consequence of nonequilibrium conditions, we obtained DSC scans at $0.2^\circ\text{C min}^{-1}$ for mixtures of composition $X_{18} = 0.31, 0.38$, and 0.40 . The onset and completion temperatures for the melting of the mixtures with molar compositions $X_{18} = 0.31$ and 0.40 were very comparable within $\pm 0.5^\circ\text{C}$, using either of the temperature-scan rates. This was not the case for the mixture of $X_{18} = 0.38$. In this mixture, although the onset temperature for the melting was the same, the completion temperature was of 41.5°C when scanning was $1.0^\circ\text{C min}^{-1}$ and 44.8°C when scanning was at $0.2^\circ\text{C min}^{-1}$. An undetected endothermic peak (indicated with an asterisk in Fig. 4) was observed above 42°C at the lower scanning rate. For the construction of the phase diagram, we used the onset and completion temperatures taken from the scans obtained at $0.2^\circ\text{C min}^{-1}$ in the case of the three selected mixtures.

The horizontal line in the phase diagram (Fig. 5) at $\sim 25^\circ\text{C}$ clearly delimits a region below which only solid phases exist. However, between this line and the liquidus line we observe other endothermic transitions, namely for mixtures of composition between $X_{18} = 0.09$ and $X_{18} = 0.95$. A solidus line, not coincident with the horizontal line at $\sim 25^\circ\text{C}$, may exist in this phase diagram at a higher temperature, but this cannot be defined from the calorimet-

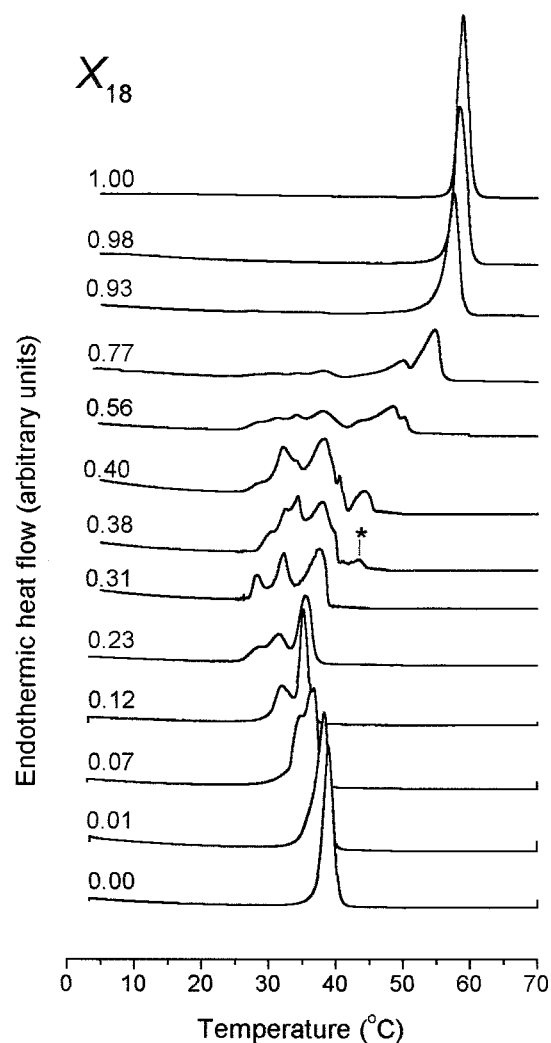


FIGURE 4 DSC heating scans for selected mixtures of 1-tetradecanol + 1-octadecanol obtained at a scanning rate of $1.0^{\circ}\text{C min}^{-1}$, excepting scans done on the mixtures of composition $X_{18} = 0.31, 0.38$, and 0.40 , which were obtained at a scanning rate of $0.2^{\circ}\text{C min}^{-1}$ (see text).

ric data. In an attempt to obtain a better definition of the compositions of the coexistent phases in the system in this region, we attempted FTIR studies on the mixtures.

FTIR-analysis of binary mixtures of 1-tetradecanol and 1-octadecanol

To follow the thermal behavior of the components individually, mixtures of the two alkanols in which one of the two components was perdeuterated were studied by FTIR. Thus, we have studied mixtures of 1-octadecanol- D_{37} with 1-tetradecanol and 1-tetradecanol- D_{29} with 1-octadecanol. Perdeuterated acyl chains have CD_2 -stretching bands in the region of 2000 to 2300 cm^{-1} well separated from the CH_2 -stretching region (compare Fig. 6 with Fig. 2), but the band associated with the CD_2 -rocking vibration in the 600 -

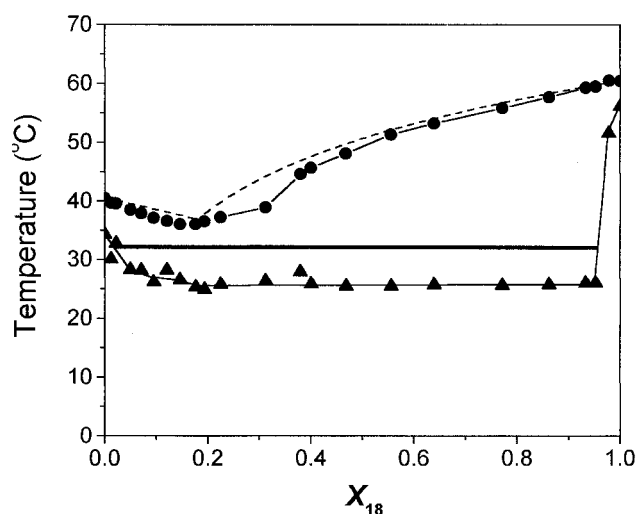


FIGURE 5 Phase diagram obtained for 1-tetradecanol + 1-octadecanol binary mixture. The points are experimentally obtained onset and completion temperatures for the endothermic transitions. The dashed lines are ideal solubility predictions for a eutectic system. The horizontal line at $\sim 32^{\circ}\text{C}$ indicates the presumed solidus, as suggested from an interpretation of the FTIR experiments (see text).

to 690-cm^{-1} spectral region (Maroncelli et al., 1985) is coincident with other CH_2 vibration bands and, therefore, difficult to analyze. On the other hand, no perdeuterated polymethylene chain vibration bands are found overlapping the CH_2 -rocking band around 710 to 730 cm^{-1} . The phase transitions of the nondeuterated alkanol and the perdeuterated alkanol in these mixtures can, therefore, be followed independently by FTIR spectroscopy, as a function of temperature, without ambiguity.

The thermotropic behavior of perdeuterated alkanols differs from that of the nondeuterated compounds primarily in the T_m , which is $\sim 4^{\circ}\text{C}$ lower for the former. Thus, binary mixtures of a perdeuterated and a nondeuterated alkanol have a thermotropism that is not exactly identical to that of mixtures of two nondeuterated compounds. However, the thermotropic behavior of a nondeuterated alkanol in a perdeuterated/nondeuterated binary mixture is probably qualitatively comparable with its behavior in a nondeuterated binary mixture. Thus, FTIR, obtained using a perdeuterated/nondeuterated binary mixture, may be used to understand, albeit in a speculative manner, the physical state of this component in nondeuterated binary mixtures.

Mixtures of composition $X_{18} = 0.50$ and 0.09 were chosen for FTIR analysis as representative of the two sides of the phase diagram in Fig. 5. Each of these mixtures was analyzed as two samples: 1-octadecanol- D_{37} with 1-tetradecanol, and 1-tetradecanol- D_{29} with 1-octadecanol. FTIR spectra were recorded as a function of temperature at intervals of 1°C , during sample heating from 10°C . The phase behavior of the nondeuterated component was monitored through changes in the frequency of the CH_2 -stretching and

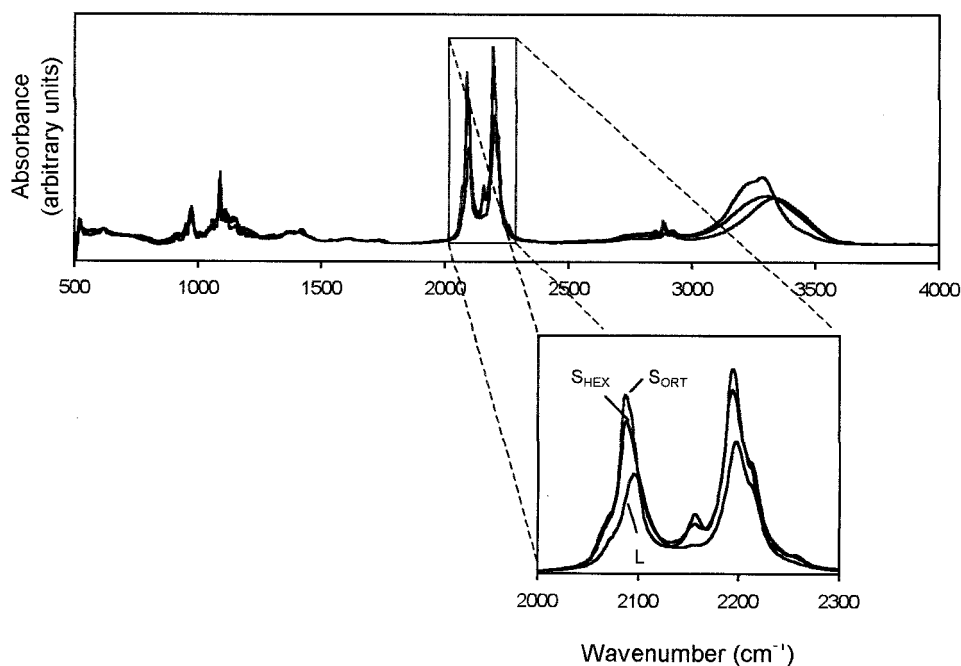


FIGURE 6 FTIR spectra of 1-tetradecanol- D_{29} in the L (41°C), S_{HEX} (33°C), and S_{ORT} (23°C) phases during a typical cooling run. The expanded figure shows the CD_2 -stretching (symmetric and asymmetric) frequency region.

CH_2 -rocking vibration bands as described earlier for the pure compounds. The phase behavior of the deuterated component was monitored through changes in the frequency of the CD_2 -stretching vibration band. The results for the complementary mixtures, of composition $X_{18} = 0.50$ are plotted in Fig. 7. It must be remembered that the deuterated compounds have a lower T_m than the nondeuterated compounds. Thus, the temperature of the liquidus in these mixtures is slightly lower when the higher melting component is perdeuterated, whereas the temperature of the solidus is slightly depressed when the lower melting component is perdeuterated. For example, the calorimetrically measured onset and completion temperatures for the endothermic transitions of binary mixtures with $X_{18} = 0.56$ were 25.3 and 51.3°C for the mixture of 1-tetradecanol + 1-octadecanol, 23.8 and 52.0°C for the mixture of 1-tetradecanol- D_{29} + 1-octadecanol, and 24.8 and 48.3°C for the mixture of 1-tetradecanol + 1-octadecanol- D_{37} .

Let us now examine the FTIR data in Fig. 7 for binary mixtures of 1-tetradecanol- D_{29} + 1-octadecanol (Fig. 7, A–C). In the melting of the mixture, the CH_2 -stretching band region of the spectrum (1-octadecanol component) shows a transition that begins at 42°C and ends at 51°C, which appears to be nonmonotonic at ~46°C (Fig. 7 A). The CH_2 -rocking vibration for the same component shows a coalescence of the vibrational bands at ~48°C (Fig. 7 C). Therefore, we conclude that a transformation of an S_{ORT} phase to an L phase occurs between 46 and 51°C. We also propose that this phase is predominantly composed of 1-octadecanol.

The CD_2 -stretching band region of the spectrum of the mixture (1-tetradecanol- D_{29} component, Fig. 7 B) shows a broad transition that initiates at ~32°C and is only completed at ~50°C. However, it must be noted that pure perdeuterated chains melt at lower temperatures than their nondeuterated homologues. This effect is likely to be dominant in the melting of a phase where the perdeuterated chain is the major species. The transition seen in Fig. 7 B can be interpreted in terms of the melting of two phases: one that begins at ~32°C (somewhat higher if perdeuteration effects are taken into account) and corresponds to the melting of a tetradecanol-rich phase and another that corresponds to the melting of the octadecanol-rich phase (Fig. 7 A) and is a small fraction of the total melt. An unambiguous assignment of the solid phase that melts to liquid 1-tetradecanol- D_{29} is not possible from this data because the CD_2 -rocking bands could not be analyzed as discussed earlier.

When the FTIR spectrum of the binary mixture of 1-tetradecanol + 1-octadecanol- D_{37} is examined (Fig. 7 D–F), a transition, beginning at 32°C and completed at ~45°C, is apparent in the CH_2 -stretching band region (1-tetradecanol component). However, the transition does not appear to be monotonic and the band-shift to higher frequencies observed between 40 and 45°C could correspond to a different phase transition. These observations agree with the nonmonotonic melting behavior of the 1-tetradecanol- D_{29} component observed in the previous mixture and discussed in the preceding paragraph. The two bands observed in the CH_2 -rocking band region (diagnostic of an S_{ORT} phase)

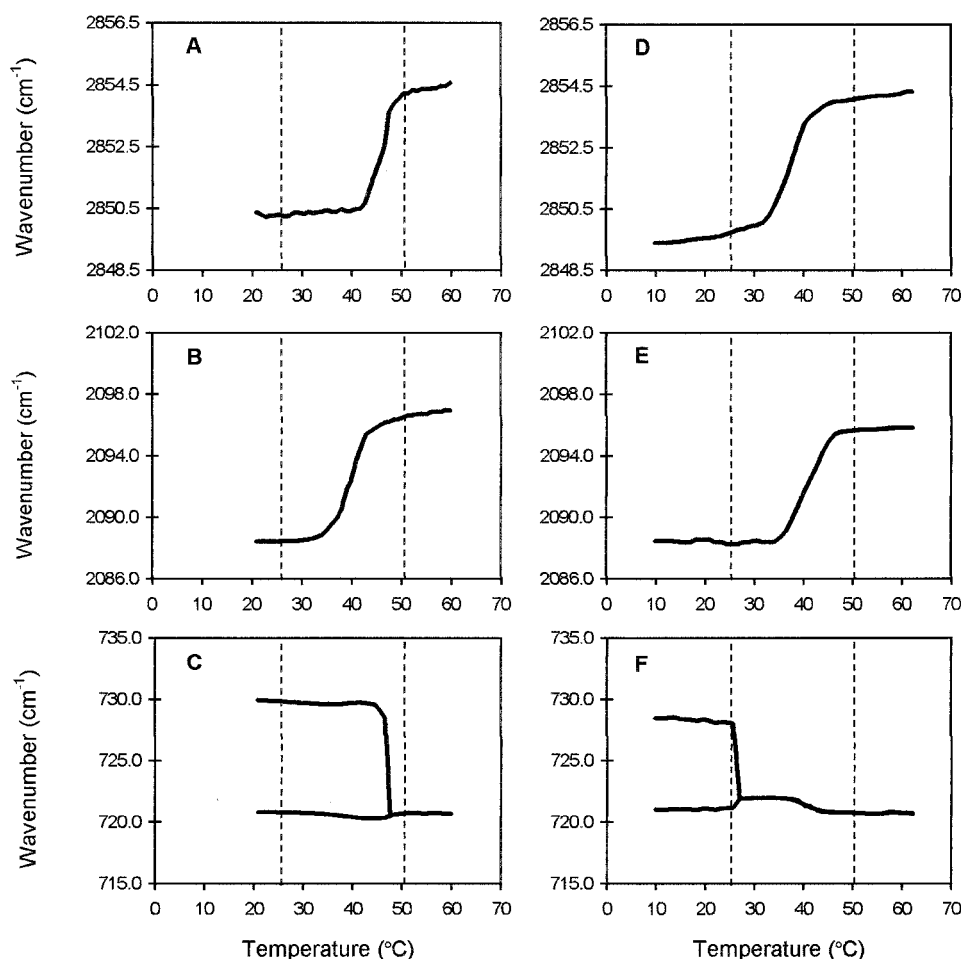


FIGURE 7 Temperature-induced changes in frequency of the CH₂-symmetric stretching, CD₂-symmetric stretching, and the CH₂-rocking vibration bands in mixtures of 1-tetradecanol + 1-octadecanol where one of the components was perdeuterated. $X_{18} = 0.50$. The results obtained for the mixture of 1-tetradecanol-D₂₉ + 1-octadecanol are plotted in A through C, and those obtained for the mixture of 1-tetradecanol + 1-octadecanol-D₃₇ are plotted in D through F. The dashed lines indicate the onset and completion temperatures for the melting of a mixture of 1-tetradecanol + 1-octadecanol of $X_{18} = 0.5$ as observed by DSC.

coalesce at 26°C, indicating the disappearance of an S_{ORT} phase composed of 1-tetradecanol at this temperature. We conclude, therefore, that the solid phase composed primarily of 1-tetradecanol, which begins to melt at 32°C, is of the S_{HEX} type and derives from an S_{ORT} phase that exists below ~25 to 26°C. The CD₂-stretching band region in the spectrum of the mixture (1-octadecanol-D₃₇ component, Fig. 7 E) clearly shows a broad transition between 35 and 46°C (which should be corrected for perdeuteration effects particularly at the higher end where a 1-octadecanol-D₃₇-rich phase would dominate the behavior seen). This transition, although overlapping the broad transition detected for the 1-tetradecanol component (Fig. 7 D), extends to the higher temperature that would be expected for an octadecanol-rich phase (discussed above in connection with Fig. 7 A).

In conclusion, it would appear that in a mixture of composition $X_{18} = 0.50$, the tetradecanol component in a S_{ORT} phase begins to transform into an S_{HEX} phase at low tem-

peratures, i.e., at ~26°C observed by FTIR and at ~25°C by DSC. For temperatures below 26°C, two S_{ORT} phases coexist: one, rich in tetradecanol, and the other rich in octadecanol. The 1-tetradecanol-enriched S_{HEX} solid phase will begin to melt at ~32°C (Fig. 7 B and D and line in Fig. 5), separately from the octadecanol component, thus defining the solidus at this temperature. At temperatures between the solidus and the liquidus, an S_{ORT} phase, predominantly composed of octadecanol, coexists with a tetradecanol-enriched liquid phase. This S_{ORT} phase melts at the liquidus.

Similar experiments with mixtures having $X_{18} = 0.09$ were also done (data not shown). The mixture composed of 1-tetradecanol-D₂₉ + 1-octadecanol did not show the CH₂-rocking vibration band splitting characteristic of an S_{ORT} phase. The CH₂-stretching (from the 1-octadecanol component) and CD₂-stretching (1-tetradecanol-D₂₉ component) vibrations showed completely coincident transitions starting at ~27° and ending at ~33°C. Considering that the phase

that is undergoing melting is predominantly composed of 1-tetradecanol-D₂₉, these temperatures would have to be corrected for the perdeuteration effect to ~ 30 and $\sim 36^\circ\text{C}$, respectively. The mixture composed of 1-tetradecanol and 1-octadecanol-D₃₇ showed the band-splitting characteristic of an S_{ORT} phase in the CH₂-rocking vibration band (arising from the 1-tetradecanol component) at low temperatures. The coalescence transition of this band, indicating a transition from an S_{ORT} to an S_{HEX} or L phase occurs between 30 and 32°C and is very clearly separated from a transition occurring between ~ 33 and 36°C detected identically in the CH₂-stretching (1-tetradecanol component) and CD₂-stretching (1-octadecanol-D₃₇) vibrational bands. The first of these transitions (S_{ORT} to S_{HEX} or L) occurs at a slightly higher temperature than indicated in the calorimetrically defined phase diagram, and the apparent completion of the second transition is somewhat lower than the calorimetrically derived liquidus line. We feel, however that this discrepancy is a result of the slope of the calorimetrically defined lines in this region of the phase diagram. Particularly at 36°C the amount of solid phase in the mixture may be so small as to make it virtually undetectable in the FTIR measurements. However, we also feel confirmed in the conclusion that a tetradecanol-rich S_{HEX} and an octadecanol-rich S_{ORT} phase coexist in the region of the phase diagram between the horizontal line, defined by DSC, at $\sim 25^\circ\text{C}$ and the solidus, proposed from the FTIR results, to lie at $\sim 32^\circ\text{C}$. In the upper left-hand region of the phase diagram, therefore, the coexisting phases would be an L phase and a tetradecanol-rich S_{HEX} phase.

DISCUSSION

The plant cuticle is a complex system that has considerable physiological relevance particularly with regard to the water economy of the plant and, as a consequence, the transport of nutrients and electrolytes between the various plant tissues. It is also important from the agricultural point of view because many xenobiotics (environmental pollutants, pesticides, and plant nutrients) are often applied to the cuticular surface and have to cross the epicuticular wax layer before being internalized into the plant. The epicuticular wax layer is usually a complex mixture of waxes, which, viewed as independent components, would exist in a homogeneous solid crystalline phase at ambient temperatures but, viewed as mixtures, are heterogeneous systems in which solid-solid and/or solid-fluid phase coexistence is to be expected. Transport properties across such a complex surface may be expected to be dependent upon the physical state of the wax layer, transport being more probable across wax phase boundaries and solid phase structural defects such as grain boundary defects or even across liquid phases that coexist with solid phases in the layer, than it is across well-ordered crystalline domains. Whereas this is theoretically to be expected, we are not aware of any systematic study that

unambiguously substantiates this supposition. It must be noted, however, that the concept is not new and some experimental work that tries to correlate transport properties with wax phase order have been reported (Riederer and Schneider, 1990; Schreiber and Riederer, 1996; Schreiber et al., 1997; Merk et al., 1998).

It is our intention to develop a cuticular model system reconstituted from the wax-free cutin of plants, isolated according to described methods (Schönherr and Riederer, 1986), and simple wax mixtures whose phase diagram has been independently determined. The concept is, then, to deposit an "epicuticular wax layer" of defined chemical properties on the cutin surface and study the transport properties of this reconstituted system with a view to correlating transcuticular transport to the known physical properties of the epicuticular wax layer. An obligatory first phase in this study is the choice and physical-chemical characterization of the wax, or wax mixture, that will serve as the epicuticular layer. This paper represents our first report in this effort. We discuss here the thermotropic mesomorphism of two long-chain *n*-alcohols both as pure compounds and as binary mixtures and the relevance of the binary mixtures as model "epicuticular waxes."

A mixture of 1-tetradecanol and 1-octadecanol was considered to be a convenient epicuticular wax model because 1) long-chain alkanols are often major epicuticular wax components in some plants (Reynhardt and Riederer, 1991, 1994; Martins et al., 1999); 2) both have convenient solubility properties necessary for the reconstitution step; and 3) both have a clearly defined phase transition behavior. In addition, the phase diagram of the binary mixture (Fig. 5) shows a liquidus and a solidus at experimentally accessible and convenient temperatures. We have studied the mesomorphism of the two compounds individually and as binary mixtures using DSC and FTIR. The phase transition temperatures obtained from the calorimetric measurements were in good agreement with values reported in the literature (Domanska and Gonzalez, 1997 and literature cited by these authors) for both the S_{ORT}→S_{HEX} and the S_{HEX}→L transitions. We were not able to detect the transition to a triclinic/monoclinic solid phase, the γ phase (Watanabe, 1961), which apparently does not occur for either of the *n*-alkanols examined in the range of temperatures scanned or in the period of time in which our analysis took place.

The exothermic thermograms of the pure alkanols showed two transitions, whereas the endothermic thermograms showed only one. However, the molar enthalpy of fusion equaled the sum of the molar enthalpies of the two transitions registered in the cooling thermograms, both in the case of 1-tetradecanol and 1-octadecanol, which is evidence that the solid-liquid transition was totally reversible. The crystallization of the alkanols into a S_{ORT} phase occurs passing through an intermediate S_{HEX} phase not usually detected during the melting. The S_{HEX} phase has been reported to be metastable (Watanabe, 1961), existing only in

a narrow range of temperature and gradually transforming into the S_{ORT} solid phase. In *n*-alkanes, the rotational solid phase appearing below the melting temperature, characterized by rigid (all-*trans*) hydrocarbon chains undergoing rotation about their long axes packed in a hexagonal crystalline subcell is also metastable (McClure, 1968). The observation of the S_{HEX} phase depends, therefore, on the kinetics of the process. We did observe that the hysteresis detected when comparing the heating and cooling of the alkanols could be slightly reduced by reducing the rate of temperature scanning, which may be an indication of the metastability of the S_{HEX} solid phase. We are currently studying the kinetics of the transformation of the S_{HEX} solid to the S_{ORT} solid for a homologous series of 1-alkanols, and the preliminary results indicate rate constants in the order of several hours to days depending upon the position of the measurement temperature relative to T_m . This will be the subject of a future report.

The phase diagram (Fig. 5) of the binary mixture (1-tetradecanol + 1-octadecanol) shows a liquidus with a minimal value around $X_{18} = 0.15$. Mixtures with less than 5% of the minor component showed only one endothermic transition for which the onset temperature decreased as the percentage of the impurity increased. At intermediate compositions, several transitions were detected below the liquidus line. The minimum in the liquidus and the general appearance of the phase diagram suggests eutectic behavior. A difference in chain lengths between the components of a mixture exceeding four carbon atoms has been suggested to result in total or partial solid state immiscibility (McClure, 1968). This kind of behavior has been observed in other binary mixtures of two *n*-alkanols (Domanska and Gonzalez, 1997), as well as in binary *n*-alkane mixtures (Hamami and Mehrotra, 1995) and *n*-alkane + *n*-alkanol mixtures (Plesnar et al., 1990; Plesnar and Bylicki, 1993).

In the phase diagram for the binary mixture of 1-octadecanol and 1-tetradecanol obtained by using DSC (Fig. 5), a line at $\sim 25^\circ\text{C}$ can be clearly defined, below which a mixture of solid phases exists. Between the liquidus and this line, there are clearly other endothermic processes, seen in the calorimetric scans (Fig. 4) whose characteristics cannot be defined by DSC alone. We have attempted a more detailed definition using FTIR spectroscopic studies on two mixtures of perdeuterated and nondeuterated components ($X_{18} = 0.50$ and 0.09). The results indicate that a solidus should be drawn at a temperature of $\sim 32^\circ\text{C}$. Below the solidus there is a coexistence of two solid phases, one of them an S_{HEX} phase rich in 1-tetradecanol and the other an S_{ORT} phase rich in 1-octadecanol. Both sides of the phase diagram between the solidus defined by the FTIR results and the liquidus defined by DSC correspond to regions of coexistence of a solid phase and the L phase. For X_{18} above the eutectic composition, the coexisting solid phase is of the S_{ORT} type. For X_{18} below the eutectic point, the solid phase coexisting with the L phase is of the S_{HEX} type. Below the

phase boundary, detected by DSC and shown in Fig. 5 at $\sim 25^\circ\text{C}$, the S_{HEX} phase present in the system above this boundary is converted to an S_{ORT} phase, so that two S_{ORT} solid phases coexist in the solid mixture below 25°C . It is difficult to reconcile the generally accepted view that the S_{HEX} wax phase is a metastable state with its observation in the phase diagram in Fig. 5 between 25 and 32°C , especially in view of the fact that we are heating the system in this case. In this regard we should also remember that the melting thermogram of 1-octadecanol, when obtained at a sufficiently low scanning rate ($0.2^\circ\text{C min}^{-1}$), shows the appearance of the $S_{ORT} \rightarrow S_{HEX}$ transition.

We have also exhaustively examined the phase behavior of this binary system in the cooling mode (data not shown). Whereas the liquidus is almost identical in both diagrams, the horizontal line seen at $\sim 25^\circ\text{C}$ in Fig. 5 (heating scans) appears at $\sim 12^\circ\text{C}$ (cooling scans) when the thermograms are obtained at comparable heating/cooling scan rates. We studied the annealing of the mixture ($X_{18} = 0.5$, composed of 1-tetradecanol + 1-octadecanol- D_{37}) at 30 and 26°C using FTIR. At 26°C the S_{HEX} phase existing in the system converted to an S_{ORT} phase after 2 h. At 30°C , however, this conversion of the S_{HEX} phase to an S_{ORT} phase was not detected over at least 24 h. This lends support to our belief that the S_{HEX} phase, between 25 and 32°C , in the diagram shown in Fig. 5 is a relatively stable state.

Judging from the results reported here for a relatively simple binary system of two chemically homologous waxes, it would appear that long-chain waxes have very complex mixing characteristics. It might even be appropriate to say that in the extremely complex wax mixture that constitutes the epicuticular wax layer, phase immiscibility is probably the rule rather than the exception. In such a complex system, even though the individual components may have melting points at very high, physiologically irrelevant temperatures as pure compounds, their existence as constituents of fluid phases at ambient temperatures cannot be excluded. In fact, several studies on epicuticular wax extracts show that at ambient temperature these waxes have coexisting crystalline and fluid phases (Reynhardt and Riederer, 1991, 1994; Schreiber et al., 1997). In any case, the solid phase immiscibility expected would tend to make the epicuticular wax layer a mosaic of phase domains even at very low temperatures. Transport across such a mosaic layer may occur through the interface between adjacent solid phases, which will necessarily have a crystalline mismatch, or by dissolution into and diffusion across fluid phases in the structure. These transport paths could be quite complex depending upon the percolation properties of the system. The transport route will also depend upon the nature of the transported molecules or ions, their dimensions, hydration states and energies, solubility in fluid wax phases, and partitioning between the external/internal aqueous phases and the wax phase.

We acknowledge the support of the program PRODEP, which permitted L. C. a leave of absence from the Universidade do Algarve, and the Ministry for Science and Technology (MCT) for financing the research reported in this paper through programs of the Foundation for Science and Technology (Fundação para a Ciência e a Tecnologia, FCT). The careful review process and the constructive criticisms of the reviewer have resulted in a significant improvement of the manuscript and are gratefully acknowledged.

REFERENCES

- Casal, H. L., D. G. Cameron, and H. H. Mantsch. 1983. Infrared spectra of crystalline *n*-alkanes: changes observed during the phase I \rightarrow phase II transition. *Can. J. Chem.* 61:1736–1742.
- Casal, H. L., and H. H. Mantsch. 1984. Polymorphic phase behavior of phospholipid membranes studied by infrared spectroscopy. *Biochim. Biophys. Acta.* 779:381–401.
- Casal, H. L., H. H. Mantsch, D. G. Cameron, and R. G. Snyder. 1982. Interchain vibrational coupling in phase II (hexagonal) *n*-alkanes. *J. Chem. Phys.* 77:2825–2830.
- Davies, M., and B. Kybett. 1965a. Sublimation and vaporization heats of long-chain alcohols. *Trans. Faraday Soc.* 61:1608–1617.
- Davies, M., and B. Kybett. 1965b. Heats of solution and of polymorphic changes in some straight chain alcohols and in hexadecanoic acid. *Trans. Faraday Soc.* 61:2646–2651.
- Domanska, U., and J. A. Gonzalez. 1997. Solid-liquid equilibria for systems containing long-chain 1-alkanols. III: Experimental data for 1-tetradecanol, 1-hexadecanol, 1-octadecanol or 1-icosanol + 1-butanol, 1-hexanol, 1-octanol or 1-decanol mixtures: characterisation in terms of DISQUAC. *Fluid Phase Equilibria* 129:139–163.
- Hammami, A., and A. K. Mehrotra. 1995. Liquid-solid-solid thermal behavior of $n\text{-C}_{44}\text{H}_{90}$ + $n\text{-C}_{50}\text{H}_{102}$ and $n\text{-C}_{25}\text{H}_{52}$ + $n\text{-C}_{28}\text{H}_{58}$ paraffinic binary mixtures. *Fluid Phase Equilibria* 111:253–272.
- Holloway, P. J. 1994. Plant cuticles: Physical chemical characteristics and biosynthesis. In *Air Pollutants and the Leaf Cuticle*. K. E. Percy, J. N. Cape, R. Jagels, C. J. Simpson, editors. NATO ASI Series, Springer-Verlag, London. 1–14.
- Kuchhal, Y. K., R. N. Shukla, and A. B. Biswas. 1979. Differential thermal analysis of *n*-long chain alcohols and corresponding alkoxy ethanols. *Thermochim. Acta.* 31:61–70.
- Maroncelli, M., H. L. Strauss, and R. G. Snyder. 1985. On the CD₂ probe infrared method for determining polymethylene chain conformation. *J. Phys. Chem.* 89:4390–4395.
- Martins, C. M. C., S. M. M. Mesquita, and W. L. C. Vaz. 1999. Cuticular waxes of the Holm (*Quercus ilex* L. subsp. *ballota* (desf.) samp.) and Cork (*Q. suber* L.) oaks. *Phytochem. Anal.* 10:1–5.
- McClure, D. W. 1968. Nature of the rotational phase transition in paraffin crystals. *J. Chem. Phys.* 49:1830–1839.
- Merk, S., A. Blume, M. Riederer. 1998. Phase behavior and crystallinity of plant cuticular waxes studied by Fourier transform infrared spectroscopy. *Planta.* 204:44–53.
- Mosselman, C., J. Mourik, and H. Dekker. 1974. Enthalpies of phase change and heat capacities of some long-chain alcohols: adiabatic semi-microcalorimeter for studies of polymorphism. *J. Chem. Thermodyn.* 6:477–487.
- Plesnar, Z., A. Bylicki. 1993. (Solid + liquid) equilibria in (hexadecan-1-ol + hexadecane). *J. Chem. Thermodyn.* 25:1301–1309.
- Plesnar, Z., P. Gierycz, and A. Bylicki. 1990. (Solid + liquid) equilibria in (*n*-octan-1-ol + *n*-hexadecane or *n*-dodecane or *n*-undecane). *J. Chem. Thermodyn.* 22:393–398.
- Pradhan, S. D., S. S. Katti, B. Kulkarni. 1970. Dielectric properties of *n*-long chain alcohols, alkoxyethanols and alkoxypropanols. *Indian J. Chem.* 8:632–637.
- Riederer, M., and G. Schneider. 1990. The effect of the environment on the permeability and composition of Citrus leaf cuticles. *Planta.* 180: 154–165.
- Reynhardt, E. C., and M. Riederer. 1991. Structure and molecular dynamics of the cuticular wax from the leaves of *Citrus aurantium* L. *J. Phys. D. Appl. Phys.* 24:478–486.
- Reynhardt, E. C., and M. Riederer. 1994. Structures and molecular dynamics of plant waxes: II. Cuticular waxes from the leaves of *Fagus sylvatica* L. and *Hordeum vulgare* L. *Eur. Biophys. J.* 23:59–70.
- Schönherr, J., and M. Riederer. 1986. Plant cuticles sorb lipophilic compounds during enzymatic isolation. *Plant Cell Environ.* 9:459–466.
- Schreiber, L., T. Kirsch, and M. Riederer. 1996. Diffusion through cuticles: principles and models. In *Plant Cuticles: An Integrated and Functional Approach*. G. Kerstiens, editor. BIOS Scientific Publishers, Oxford, UK.
- Schreiber, L., and M. Riederer. 1996. Determination of diffusion coefficients of octadecanoic acid in isolated cuticular waxes and their relationship to cuticular water permeabilities. *Plant Cell Environ.* 19: 1075–1082.
- Schreiber, L., K. Schorn, and T. Heimburg. 1997. ²H-NMR studies of cuticular wax isolated from *Hordeum vulgare* L. leaves: identification of amorphous and crystalline wax phases. *Eur. Biophys. J.* 26:371–380.
- Watanabe, A. 1961. Synthesis and physical properties of normal higher primary alcohols. IV. Thermal and X-ray studies on the polymorphism of the alcohols of even carbon numbers from dodecanol to tetratriacontanol. *Bull. Chem. Soc. Japan* 34:1728–1734.